# Building Damage Detection to the 2008 Wenchuan Earthquake by Fusing the High-resolution SAR and Optical Images

X. Chen [a, *], J. Zhang [a], L. An [a]

[a] Institute of Crustal Dynamics, China Earthquake Administration, No.1 Anningzhuang Road, Beijing, China-
chenxioffice@126.com

**ABSTRACT:**

High-resolution optical and SAR images are fused to detect the earthquake damage for the 2008 Wenchuan earthquake. First, all the images should be projected and registered in a united geo-reference to get a superposition building ground features. The quantitative correlation coefficient from an Envisat ASAR image series was used as a rapid and direct way to get the degree of change in ground surface objects. Then the parts edges of building were extracted with the help of the Object-Oriented classification results from aero optical images. To explore the relationship between the damage of the man-made objects and the disaster source, several scattering transform models of the damaged objects were analyzed with the geological background. Using the overlay tools in GIS, we could detect the damaged part of buildings. The result showed that the heaviest damage, such as collapse and distortion, had a large decrease in correlation and was mainly distributed near the rupture.

## 1. INTRODUCTION

As the huge earthquake, such as 2008 Wenchuan earthquake, would destroy a large area with a complex rupture mechanism, it is rather hard to quantitatively assess the degree and distribution of damage, especially while the communication and traffic are interrupted. Although field investigation, such as analyzing the seismic damage grade of different kinds of buildings to assess an area's level of damage, is still the trustiest method for seismic disaster assessment, remote sensing techniques could rapidly, directly obtain the conditions of disaster areas for emergency response and rescue using less human and material resources. Some well known technics of building boundary extraction have already been proposed in the fields of optical imagery in previous papers and have proved to provide efficient results for normal structure building. But the building damaged by the earthquake generally has anomalous shape and texture which make it hard to perform the anticipant result in seismic cases.

A hot research topic is to understand information on seismic damage to buildings based on the scattering of electromagnetic waves, and then develop quantitative models. The correlation of the radar echoes pre- and post-earthquake from the same area could help us to observe the quantitative change of man-made objects on the ground. Both the amplitude information (Aoki, 1998; Yonezawa and Takeuchi, 1998) and the phase information (Yonezawa and Takeuchi, 1999) of SAR images are useful to find the distribution of building damage. In order to find a quantitative relationship between the seismic damage levels and microwave backscattering characteristics of buildings, M. Matsuoka and F. Yamazaki (1999, 2000) analyzed the difference in backscattered intensity, intensity correlation and complex coherence of pre- and post-event SAR image series for earthquake-hit areas with ground truth data. As accuracy of the conclusions based on the complex coherence is easily influenced by satellite geometry, acquisition duration, and wavelength of radar (A. Zebker 1992), C. Yonezawa and S. Takeuchi (2001) advanced the backscattering coefficient of the ground surface for seismic damage assessment. Hence, M. Matsuoka and F. Yamazaki (2003, 2004a, 2004b, 2006, 2007) developed a quantitative discrimination function based on the difference of the backscattering coefficient and correlation coefficient to detect areas of building damage and used the method on SAR image series of the Hokkaido Earthquake in 1993, Kobe Earthquake in 1995, Kocaeli Earthquake in 1999, Gujarat Earthquake in 2001, Bam Earthquake in 2003, Niigata-ken Earthquake in 2004, and Yogyakarta and Central Java Earthquake in 2006. Y. Dong (2010) performed absolute radiometric calibration for SAR products to derive the backscattering coefficient sigma nought from an image digital number (DN) value of the 2008 Wenchuan earthquake to get a more accurate result.

Although strongly dependent on observation conditions, considering the practical acquisition of damage conditions under the time requirement, it is more feasible to use the correlation coefficient than other indexes (M. Matsuoka, 2007). E. J. Fielding (2005) discussed several physical and geological factors for decorrelation and used the result for detecting building damage and surface rupture in the Bam earthquake. S. Stramondo (2006) improved the damage classification method by combining it with optical images. Y. Jin (1993) summarized electromagnetic scattering modeling for quantitative remote sensing.

In this paper, we use the change value of correlation coefficient to assess the damage degree of important buildings. In order to localize the man-made area, as the vegetation, bareland and water area would affect the statistical result, and even represent an increasing trend in correlation. Stramondo (2006), Trianni (2008), and Y. Dong (2011) appended GIS data and high spatial resolution optical images for block mapping.

---

* X. Chen. No. 1, Anningzhuan Road, Beijing 100086, China. Tel: (010)62846725 E-mail:chenxioffice@126.com

## 2. DECORRELATION MODEL FOR DAMAGE BUILDINGS AND IMPROVEMENT BY OPTICAL IMAGES

### 2.1. Basic theory and model

As a multi-temporal and single-angle remote sensing technique, the most popular method is change detection by scattering correlation. Seismic damage would affect the strength of a radar backscattering signal, which reflects the change in roughness of the surface, the moisture level of the area and the incident angle of the microwave. The correlation, which is calculated from the phases of the backscattering echoes using two co-registered complex SAR images for different times, is a suitable and sensitive parameter for change detection. The correlation coefficient $|\gamma|$ of pixels in the same position in images is calculated as a weighted spatial average over a window of size N (Hagberg, 1995; Rosen, 1996):

$$| \gamma |=| \frac{|\mathbf{S}_{12}|}{\sqrt{\mathbf{S}_{11}}\sqrt{\mathbf{S}_{22}}} \qquad (1)$$

Where

$$\mathbf{S}_{12} = \sum_{k=0}^{N-1} \sum_{j=0}^{N-1} w_N(k,j)\mathbf{S}_1(k,j)\mathbf{S}_2^*(k,j)\mathbf{S}_D(k,j) \quad (2)$$

$$\mathbf{S}_{11} = \sum_{k=0}^{N-1} \sum_{j=0}^{N-1} w_N(k,j)\mathbf{S}_1(k,j)\mathbf{S}_1^*(k,j) \qquad (3)$$

$$\mathbf{S}_{22} = \sum_{k=0}^{N-1} \sum_{j=0}^{N-1} w_N(k,j)\mathbf{S}_2(k,j)\mathbf{S}_2^*(k,j) \qquad (4)$$

And $S_1(k, j)$ is the value of the pixel on row k, column j, in the first SAR image. The same is true for $S_2(k, j)$ in the second SAR image. * implies a complex conjugate, $w_N$ is the scalar weighting array of the window, and $S_D$ is a complex parameter used to detrend the interferometric phase in the window, removing a local phase slope which would otherwise bias the correlation estimate. In this paper, the value of N is 5. For a completely coherent radar scatterer that does not change between radar observations, the correlation is 1. If the scatterer is completely different between the two observations, the value is 0.

Some typical decorrelation cases are summarized from former papers (M. Matsuoka, F. Yamazaki 2005; Y. Dong, 2011). 1) Open spaces or collapsed buildings have lower reflectance because microwaves are scattered in different directions. 2) The correlation coefficient is reduced as the irregularity of the ground surface changes due to landslides and slope failures. 3) Specular reflection happens on flat roofs and produces a weak backscattering. 4) Double-bounce reflection happens between building walls and the ground and produces a strong backscattering, while single-bounce reflection happens on tilted roofs facing the radar beam and produces stronger backscattering. 5) Water absorbs microwaves. In general, there are three kinds of element models causing the decorrelation.

1) The surface shape change causes the scattering path to change (Fig. 1, Fig. 2). As the angle of the building roof changes, or nearby objects form new parts of the building, the backscattering signal changes its direction and intensity.

2) Structural collapse makes single-bounce scattering change to different directions (Fig. 3). The height and structural change create a new roughness interface instead of the old flat one. So simple surface backscattering was transformed into anomalous volume scattering.

3) The change of interface material transforms absorption and backscattering (Fig. 4, Fig. 5). The most common factor is water.
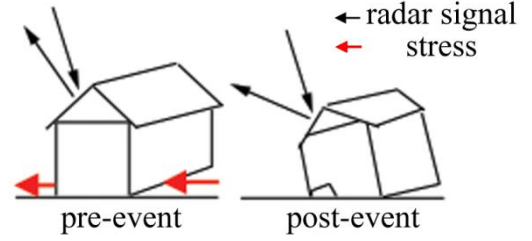


Figure1. Leaning of scattering interface. The building would change the shape of the roof, which makes the radar signal change the backscattering direction.
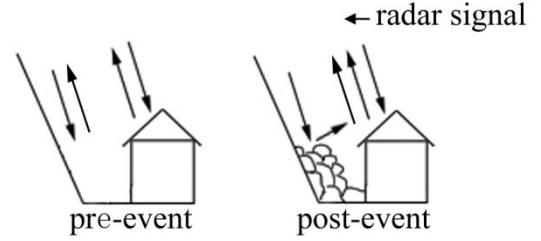


Figure 2. Expansion of scattering interface. Because of accumulation due to the landslide, the scattering intensity would increase.
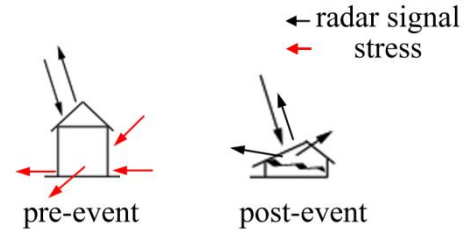


Figure 3. Building collapse. The surface backscattering is transformed to the anomalous volume scattering.
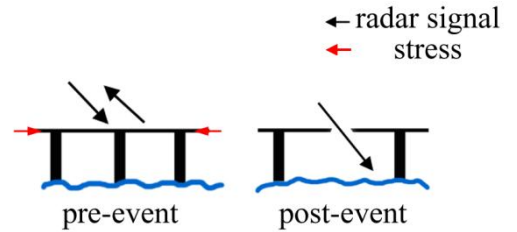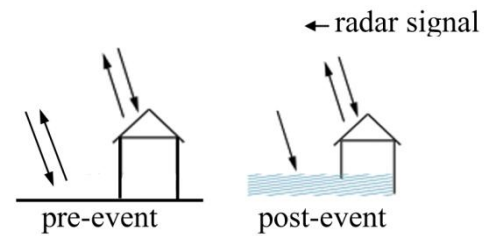


Figure 4. Broken bridge. The signal which penetrates the hole would be absorbed by the water.



would be absorbed by the water.

For the value of pixels in the result images, the decrease is related to the damage level (M. Matsuoka and F. Yamazaki, 1999, 2000, 2003, 2004a, 2004b, 2005). While analyzing the relationship between the correlation change and the damage rank, they classified the pixels that correspond to the area of each damage rank selected from the SAR images and found that the distribution intervals of the change value went up as the damage level was higher.

One or more cases could occur with a single object. The damage performs like a pulse signal and could effectively change the value of the pixel. So decorrelation could tell us the possibility of seismic damage. The integration effect is a key problem. As a pixel is affected by plenty of objects at different scales, the sum of the intensity may increase or decrease, so an increase in correlation may happen to many statistical samples. But in most heavy damage cases, the correlation would decrease, which was validated by field investigation.

### 2.2. Data processed

We propose to fuse the high-resolution optical and SAR images based on the correlation coefficient in order to detect the earthquake damage for building as follow steps. First, all the images should be projected and registered in a united geo-reference to get a finer superposition building ground features. And then, the correlation coefficient of pre- and pre-earthquake SAR image pairs subtracted the correlation coefficient of pre- and post-earthquake SAR image pairs in order to detect changes in the man-made area due to seismic damage. As rescue time is limited, the SAR images were not pre-processed by radiometric correlation.

In order to improve the comprehensibility of the correlation image with speckle, we fuse the image with the high resolution optical image taken after the earthquake. After image segmenting, we got the polygons as basic damaged element. Now we got the elements and sub elements for recognizing the earthquake damage to the building. Using the overlay tools in GIS, we could detect the damage by two factors: area and number of the sub elements. The buildings whose most elements have the high value would be judged as damaged building.

### 3. THE CASES IN WENCHUAN EARTHQUAKE

According to the China Earthquake Networks Center, on May 12, 2008, the Wenchuan earthquake, with a magnitude of Ms 8.0, struck in southwestern China. The earthquake caused over five million buildings to collapse and damaged 21 million across a wide area (US Geological Survey, 2008). It also led to a mass of landslides and rock falls, some of which dammed rivers, forming 3,000 barrier lakes and causing further building damage. The mainshock hypocenter was located about 30 km southwest of Yingxiu (31.061°N, 103.333°E) at a 19-km depth and had a thrust mechanism with a right-lateral slip component (USGS, 2008). The peak of coseismic surface deformation on the Beichuan Fault is found near the town of Beichuan (X. Xu, 2009). Because of the tectonic condition, the dynamic mechanism caused heavy damage to Beichuan with multiple forms of damage cases. The town of Beichuan was therefore chosen as our research area. The data we chose included a aero optical image and Envisat ASAR radar data. The ASAR data were processed from raw data. The basic information of the ASAR data is in Table 1.

| Track | 018 | | |
|---|---|---|---|
| Acquisition date | 08-Feb-06 | 15-Nov-06 | 28-May-08 |
| Orbit Type | descending | descending | descending |
| Pixel size of range /m | 7.8 | 7.8 | 7.8 |
| Pixel size of azimuth /m | 4 | 4 | 4 |

Table 1. Parameters of the ASAR data used in the process.

The demonstration area was former Beichuan (E104.44°~104.47°, N31.82° ~31.85°). The pixel value of the correlation image (Fig. 6) represents the decrease in the correlation coefficient. Through statistical analysis (Fig. 7), the mean value was 0.017756. So due to the earthquake, the correlation in Beichuan decreased, which accorded with the conclusion in the previous paper.
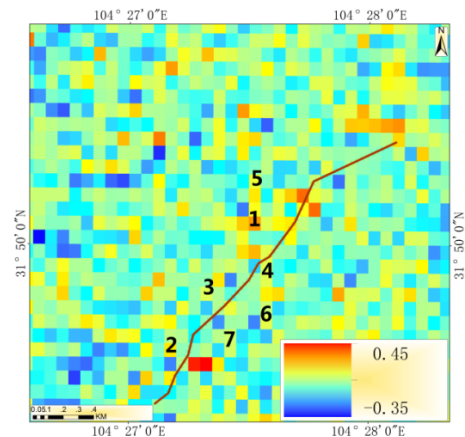


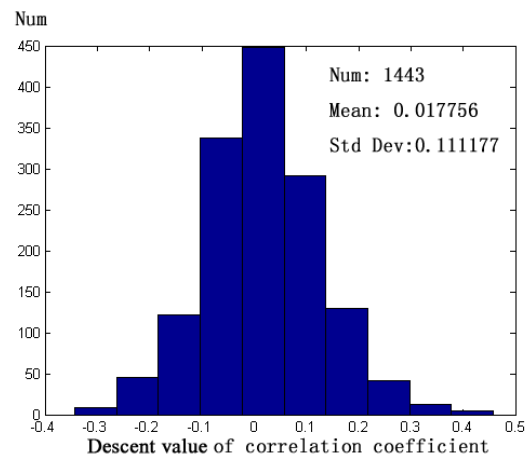Figure 6. Result of correlation decrease. The objects are indicated by the number.



Figure 7. The statistical histogram of the pixel decorrelation value in Beichuan

| ID | Decrease in correlation coefficient |
|----|-------------------------------------|
| 1  | 0.314575 |
| 2  | 0.218009 |
| 3  | 0.126538 |
| 4  | 0.131590 |
| 5  | 0.154835 |
| 6  | 0.135676 |
| 7  | 0.102144 |

Table 2. Each value of the object pixels.

## 3.1. Field Investigation

The open air museum of the Wenchuan earthquake ruins in Beichuan provided us the opportunity to investigate the relationship between the theoretical result and the degree of damage. In order to get the corresponding objects, edge vectors, which was extracted from high resolution aero optical images (Fig 8) by Objected-Oriented classification, was overlapped to the correlation image (Fig 9). The accuracy of the proposed method was validated by comparing the result of calculation with the ground investigation. Some pixels are listed in Table 2. As the deflective error in general, the data values were normalized and only used to see the deformation trend. The objects were classified into two classes: direct damage and secondary damage.



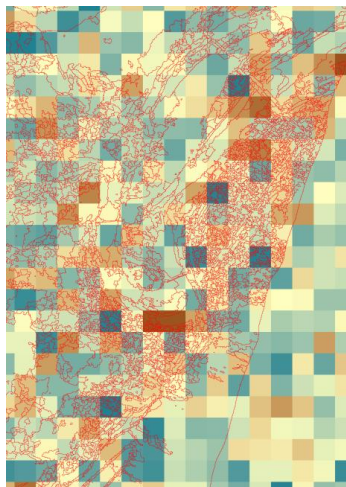Figure8. The post-earthquake aero optical image.



Figure9. The object-vectors extracted from the aero optical image.

### 3.1.1. Direct damage:
Direct damage is commonly caused by surface ruptures. Besides co-seismic ruptures such as the surface ruptures along active faults, there are sub-deformations and post-deformations including ridges, overlapping, and horizontal displacements on roads and buildings, which are formed by local stress from the abrupt energy released through the activity of the faults (J. Pei, 2009). Building damage is mainly aggravated by landform variation including the widening of mountains and the narrowing of valleys related to multilayer detachment initiated by the process of stress release and strain recovery during the quake.

So these areas extracted from the geological information would have a significantly decreased correlation coefficient.

1) Collapse. This heaviest damage pattern was mainly found near the fault rupture, such as case 1 (Fig. 10) and case 2 (Fig. 11). The corresponding pixels had the most-decreased correlation coefficient values in our cases: 0.314575, 0.218009 (Table 2). This indicated that the open spaces or collapsed buildings had rather lower reflectance because microwaves are scattered in different directions, which are typical examples of condition 2, leaning (Fig. 3). An interesting case was case 3 (Fig. 12). Only the first floor of the damaged building collapsed, while the higher floors still kept their surface shape. This condition was very hard to be identified through the pre-earthquake optical images because of the view angle. Although the change value of 0.126538 was not as high as other collapsed buildings', such as cases 1 and 2 (Table 2), the value was high enough to recognize the damage from the surrounding pixels.

2) Leaning. Specular reflection happens on flat roofs and produces a weak backscattering. So the correlation would decrease when the corresponding building leans, such as case 4 (Fig. 13), the Qushan School, which is a typical example of condition 1 (Fig. 1). But this condition is easily mistaken with surroundings noise. The result needed to be verified by other data, such as LiDAR.

3) Distortion. This condition usually happens along roads and bridges, such as case 5 (Fig. 14, Fig. 15).

The narrowing of valleys related to multilayer detachment is initiated by the process of stress release and strain recovery from the fault rupture, which is a typical example of condition 3 (Fig. 4). In Fig. 15 we can observe the raised distortion of the bridge from stress.

### 3.1.2. Secondary damage:
As the damage intensities of buildings varies remarkably along with various secondary damage, such as landslide, land collapse, seismic liquefaction of saturated soils, and quake-wave direction (J. Zhang, 2009), the cases should be inferred by surroundings.

1) Landslide. Double bounce reflection happens between building walls and the ground, which produces a strong backscattering. So the correlation coefficient would be reduced as the irregularity of the ground surface changed due to landslides and slope failures, such as case 6 (Fig. 16), which is happen near a mountain edge area.

2) Barrier Lakes. Water absorbs microwaves, which makes corresponding pixel values decrease, such as case 7 (Fig. 17), a typical example of condition 3 (Fig. 5). This condition should be validated by river vectors and optical images, as penetrative

microwaves can be easily misled by wet soil, especially after rain and flooding.



Figure10. Case 1. Collapsed buildings. Before the earthquake this was the Agriculture Bank of China, Beichuan Sub-branch.



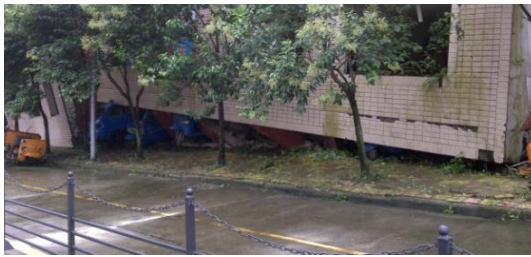Figure11. Case 2. Collapse of building groups in the south of the town.



Figure12. Case 3. The first floor of the building collapsed in the earthquake, but the higher floors still kept their surface shape.



Figure13. Case 4. Leaning building. The building is Qushan School, which is next to the Beichuan Police Station.
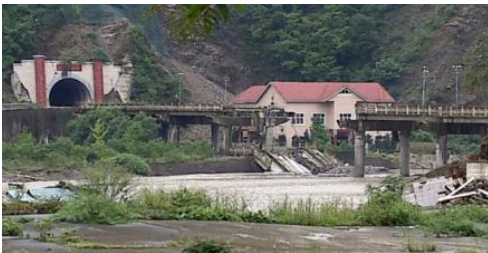


Figure14. Case 5. Xiayu Bridge, broken because of distortion from valleys.



Figure15. Case 5. Xiayu Bridge, broken because of distortion from valleys.



Figure16. Case 6. Xiayu Bridge, broken because of distortion from valleys.



Figure17. Case 7.Landslide near the bend of the Jianjiang in the town.

## 3.2. Accuracy and precision

The estimated damage distribution from SAR images almost corresponded to the results of our field survey. In spite of these results regarding the mean characteristics of SAR images, a large degree of randomness existed. While the lowland areas had good phase coherence, the phase recovery was less robust in the mountainous areas. Some part of the lower coherence was due to a combination of landslides, temporal decorrelation from vegetation, and inadequate topographic phase correction in the area of extreme relief. In the mountainous areas, there are cases which were difficult to detect due to the imaging geometry, depending on their locations, due to the influences of lay over, foreshortening, and shadow effects peculiar to SAR images.

## 4. CONCLUSION

When faced with a huge disaster like the Wenchuan earthquake, it is rather difficult to acquire a result for the damage degree distribution in a short time. The decreasing correlation

coefficient value based on SAR remote sensing techniques provides us a direct method to solve the problem.

Broad zones of decorrelation have been observed around fault ruptures after the earthquake. Combining other information, such as edge vectors of man-made object from the Object-Oriented classification result using optical images, it is possible to map changes due to the destruction of built structures. By adding the background from geological and physical geography as prior knowledge, we could get more quantitative and precise earthquake damage information for building damage based on the change in correlation. As the damage level increases, the decreased value of the correlation coefficient would also increase. Although we have a quantitative decorrelation result, the recognition of building damage is still half-quantitative and needs the help of some prior knowledge and supplementary results. However, it is enough to rapidly assess the damage degree distribution.

This method is not only a useful reference for a subsequent field survey independent of weather conditions and sun illumination, but also a powerful quantitative analysis tool for finding the distribution of damage to man-made areas and the surface ruptures, which supports recovery activities and restoration planning after such a huge earthquake.

## 5. REFERENCES

Bitelli, G., Camassi, R. and Gusella, L., 2004. Image change detection on urban area: the earthquake case. Proceedings of International Society for Photogrammetry and Remote Sensing XXth Congress. CD-ROM, No. 692:6.

Buckley, S., and abridged by Rosen, P. and Persaud, P., 2000. ROI_PAC Documentation Repeat Orbit Interferometry Package. CSR, UT Austin, USA.

Chen, X., Zhang, J., An, L.,2011 (contribution). Quantitative model for seismic damage assessment in the 2008 Wenchuan earthquake by decorrelating a SAR image series. International Journal of Digital Earth.

Chesnel, A. L., Binet, R. and Wald, L., 2007. Quantitative Assessment Of Building Damage In Urban Area Using Very High Resolution Images. Urban Remote Sensing Joint Event, 1-5.

Dong, Y., Li, Q. and Dou, A., 2010. Extracting damages caused by the 2008 Ms 8.0 Wenchuan earthquake from SAR remote sensing data. Journal of Asian Earth Sciences, 40:907-914.

Fielding, E. J., Talebian, M. and Rosen, P. A., 2005. Surface ruptures and building damage of the 2003 Bam, Iran, earthquake mapped by satellite synthetic aperture radar interferometric correlation. Journal of Geophysical research, 110:1-15.

Massonnet, D. and Feigl, K., 1998. Radar interferometry and its application to changes in the earth`s surface. Review of Geophys, 36:441–500

Matsuoka, M. and Yamazaki, F., 2004. Building Damage Detection Using Satellite SAR Intensity Images for the 2003 Algeria and Iran Earthquakes. Geoscience and Remote Sensing Symposium, 2004 IEEE International.

Matsuoka, M. and Yamazaki, F., 2004. Use of satellite SAR intensity imagery for detecting building areas damaged due to earthquakes. Earthquake Spectra, 20(3), 975-994.

Matsuoka, M. and Yamazaki, F., 2005. Building Damage Mapping of the 2003 Bam, Iran, Earthquake Using Envisat/ASAR Intensity Imagery. Earthquake Spectra, 21(S1), 285-294.

Matsuoka, M. and Yamazaki, F. and Ohkura, H., 2007. Damage mapping for the 2004 Niigata-ken Chuetsu earthquake using Radarsat images. 2007 Urban Remote Sensing Joint Event: 1-5.

Pei, J., Li, H. and Si, J., 2009. Surface Building Deformation Caused by Wenchuan Earthquake (Ms 8.0) And Its Tectonic Implication. (In Chinese) Quaternary Sciences, 29(3): 513-573.

Stramondo, S., Bignami, C. and Chini, M., 2006. Satellite radar and optical remote sensing for earthquake damage detection: results from different case studies. International Journal of Remote Sensing, 27(20): 4433-4447.

Yonezawa, C. and Takeuchi, S., 2001. Decorrelation of SAR data by urban damages caused by the 1995 Hyogoken-nanbu earthquake. International Journal of Remote Sensing, 22(8):1585-1600.

Zebker, A. and Villasenor, J., 1992. Decorrelation in interferometric radar echoes. IEEE Transactions on Geoscience and Remote Sensing. 30(5):950-959.

Zhang, J., Tang, R. and He, B, 2009. Probing on Characteristics mechanism of Disasters Caused by Wenchuan Earthquake. (In Chinese) Quaternary Sciences, 29(3): 565-523.